Facet-resolved electrochemistry: from single particles to macroscopic crystals

Song Zhang[a], Simone Ciampi[*,a]

Addresses

[a]School of Molecular and Life Sciences, Curtin University, Bentley, Western Australia 6102, Australia

*Correspondence: simone.ciampi@curtin.edu.au

Keywords: heterogeneous electrochemistry, interfaces, semiconductor electrochemistry, conductive atomic force microscopy, electrocatalysis

Abstract. Optimizing the kinetics and energy requirements of electrochemical reactions is central to the design of redox systems whose function ranges from energy conversion, to chemical catalysis and sensing. This optimization takes often the form of a trial-and-error search for the optimal electrode material. Recent research has revealed pronounced facet-dependent electrical conductivity, redox reactivity and electro-adsorption for a range of semiconductors, including silicon, Cu_2O, GaAs, InN, Ag_2O, and β-Ga_2O_3. This review critically analyzes studies which suggest that testing alternative crystal cuts of the same material can be an efficient as well as effective electrode-optimization process. We analyze these recent reports to define what is known unambiguously, and when there are contrasting views, we explore the assumptions that underlie them.

Introduction

Electrochemistry is a broad and rapidly evolving discipline, but at its core remains the branch of chemistry combining the study of electronic conduction in solids with that of ionic conduction in electrolytes [1,2]. Its ultimate aim is that of predicting and possibly engineering electrode kinetics and/or equilibrium positions of redox processes [3,4]. It follows that most progresses in electrochemistry have resulted from improvements in the understanding of the physical and chemical properties of electrified interfaces [5-7]. From sensing to energy conversion, optimizing the kinetics of an electrode reaction and engineering its

thermodynamics often begin a systematic change to the chemical nature of the electrode. For instance, volcano plots in hydrogen electrocatalysis are an excellent reminder that the nature of the electrode can dominate electrode kinetics [8]. However, the search for optimal electrode materials remains often a trial-and-error process.

Recent research has brought back attention to the scope of confining this search to a narrow range of alternative materials: alternative crystal cuts of the same material. Simply by selecting alternative crystal facets of a given material it is possible to substantially alter surface energies [9], electron trapping efficiencies [10], surface charges [11], electrode propensity to corrode [12], and adsorption selectivity [13]. Hence, facet-resolved electrochemical research is rapidly gaining momentum, especially in the fields of nanocrystals sensing [14,15], semiconductor electrochemistry [16-18], and electro- and photo-catalysis [19-22].

In this short review, we critically analyze recent research that has explored differences in electrochemical reactivity between different facets of the same metal or semiconductor. We highlight the most promising features of this emerging topic, as well as present systems where the scope of this approach is undoubtedly poor, or still unclear.

Facet-dependent electrical conductivity links to electrochemical reactivity

Silicon continues to be the technologically most relevant material [23]. With only few exceptions [24-26], silicon electrochemical research has so far focused mainly on only two silicon orientations: ⟨111⟩ and ⟨100⟩. This changed in 2017, when Huang and co-workers discovered the high electrical conductivity of Si(211) [27]. Similarly, remarkable differences between different facets of the same material are also emerging for other semiconducting materials, such as Cu_2O, GaAs, InN or Ag_2O [28-31]. Focusing on silicon and with the aid of conductive atomic force microscopy (C-AFM), it has been demonstrated that the conductivity of a junction between oxide-free silicon and a metal contact decreases in the order ⟨211⟩ >> ⟨110⟩ > ⟨111⟩ [25]. One of the most notable, and unexpected, electrochemical consequences of this facet-dependent (electrical) conductivity is to allow the silica–silicon redox couple become reversible on highly conductive Si(110) defects, which are ubiquitous on a nominal Si(111) wafer [16].

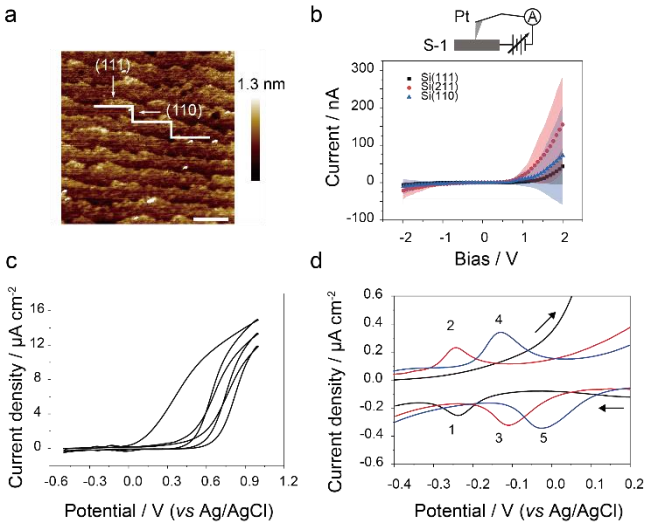

Figure 1. Facet-dependent conductivity on silicon crystals and electrochemical signatures of reversible silica–silicon conversion on highly conductive planes. (a) AFM topography image of a Si(111) wafer. Data obtained ensuring a parallel alignment between the original wafer major flat, indicating the [110] direction, and the x-direction of the AFM raster scan. Steps between terraces, here roughly parallel to the sample major flat, are ⟨110⟩ facets. The scale bar is 400 nm. (b) Schematics of a Pt–organic monolayer–Si junction in a C-AFM measurement and the corresponding I–V curves (average of 400 curves) for Si(111), Si(211) and Si(111) samples. **S-1** indicates the substrate is coated with a protective monolayer of 1,8-nonadiyne. (c) Cyclic voltammograms (CVs) of Si(111) electrodes (**S-1**), with the bias ramped from an initial −0.5 V to an anodic vertex of 1.0 V (0.1 V/s, aqueous 1.0 M $HClO_4$). (d) Magnified views of the first three sequential CV cycles (six segments) shown in (c). (a,c,d) Reprinted with minor changes from Ref. [16], copyright (2021), with permission from the American Chemical Society. (b) Reprinted with minor changes from Ref. [25], copyright (2021), with permission from the American Chemical Society.

This finding is surprising in several ways. Firstly, the notion that single crystals are an idealization is not sufficiently widespread, and its practical implications not entirely appreciated. Even a perfectly etched Si(111) wafer, of sub-nanometer roughness [32], exposes an array of vertical steps separating adjacent ⟨111⟩ terraces (Figure 1a). These steps are often aligned with the ⟨211⟩ and ⟨110⟩ directions [16]. Both Si(211) and Si(110) are more conductive than both Si(111) (Figure 1b) and Si(100), the other common silicon electrode material [25,33,34]. On these steps, and for thin oxide films only, the electrochemical silica-to-silicon conversion occurs reversibly at room temperature (Figure 1c,d). Traces amount of OH^- and O_2^- migrate through the oxide layer covering highly conductive ⟨110⟩ and ⟨211⟩ terraces separating Si(111) planes, allowing the redox reaction to proceed reversibly [16]. In fact, deliberate anodic damaging of an initially oxide-free Si(111) electrode (Figure 1c) leads to the appearance of a surface-confined cathodic wave. This wave, labelled in Figure 1d as **1** in the return segment of the first cycle, is coupled to a new anodic signal (**2**) visible in the anodic

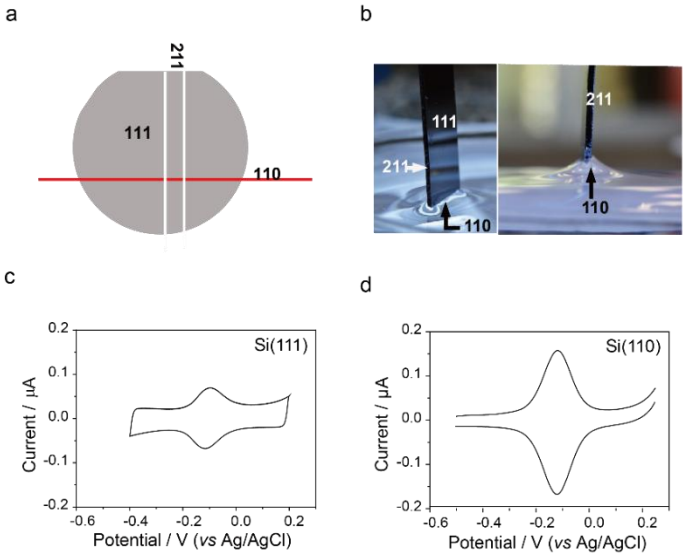

Figure 2. Macroscopic facet-resolved electrochemistry. (a) Graphical depiction of the ⟨110⟩ and ⟨211⟩ crystal directions in commercial Si(111) wafers. (b) Hanging meniscus configuration to wet exclusively the Si(110) facet, exposed by cleaving a Si(111) wafer along a direction parallel to the wafer's lap. (c,d) CVs of anodically damaged monolayer-coated Si(111) and Si(100) electrodes (0.1 V/s, aqueous 1.0 M $HClO_4$). The surface coverage of the Si/SiO*x* signal observed on Si(110) is ~ 6.9 times larger than on Si(111). The measured (capacitance) area ratio between Si(111) and Si(110) is 1.9. Reprinted with minor changes from Ref. [16], copyright (2021), with permission from the American Chemical Society.

segment of the second cycle [16].

In general, the electrochemical reduction of bulk silica, due to its high electrical resistance, is obviously of limited viability. It requires molten-salt reactors and temperatures in excess of 850 °C [35]. While these recent findings for Si(211) and Si(110) cannot immediately translate to a room-temperature bulk electrosynthesis of silicon form silica, they are however of practical importance as they explain the origin of recurrent parasitic signals often observed with silicon electrodes (Figure 1d). Unlike for platinum, gold and carbon, where all common adventitious electrochemical signals have been satisfactorily assigned and explained, the origin of common parasitic signals has remained more elusive in silicon voltammetry [36-38]. In essence, highly conductive silicon defect defines for silicon the potential window free from redox parasitic signals, and as such, suitable for the study of surface reactions by electroanalytical methods.

Furthermore, this example of nanoscopic facet-resolved electrochemistry can be scaled to relatively large electrodes (Figure 2). It is customary for silicon manufacturers to mark wafers with a lapped edge. For Si(111) wafers this edge generally marks the ⟨110⟩ direction (Figure

2a). In conjunction with readily available crystallographic stereographic projections, such lap helps in cleaving a commercial wafer to expose specific planes. For instance, cleaving the wafer in direction parallel to the lap will expose Si(110). Cyclic voltammetry in an hanging meniscus setup, such as to wet only the Si(110) facet (Figure 2b), leads to redox parasitic waves (the silica/silcon couple) significantly larger than what normally observed with Si(111) (Figure 2c,d).

Unlike for a redox reaction that requires migration of oxygenated species, like the one discussed above, or as for bias-dependent adsorptions as discussed in the next section, if the redox entity is held at some distance above the electrode, significant changes in substrate conductivity are not reflected by measurable changes in electrode kinetics. For example the charge-transfer rate constant for ferrocene molecules tethered on the top of a ~1nm-thick organic monolayer are indistinguishable between Si(111), Si(211) and Si(110), thought these surfaces have very different surface conductivities (Figure 1b) [25].

Facet-dependent effects on electro-adsorption reactions

Chemists, material scientists and engineers appreciate that the shape and size of an inorganic particle can define its reactivity [22], its catalytic behaviour [39], its ability to store or conduct charge [40], or its interactions with light [41]. Nonetheless, shape-control of nanoparticles is often serendipitous, and most generally achieved by chemical means (Figure 3a). Recently it was demonstrated that it is possible to use surface electric fields to modulate anisotropic interactions between additives and surfaces, hence predictably exploiting electrostatics to engineer the shape of nanocrystals [28,42]. There is a relationship between bias-dependent isothermal adsorption of halide ions and changes to the surface energy of Cu_2O particles, hence their crystal shape (Figure 3b). Most importantly, the sigmoidal nature of adsorption isotherms means that exceedingly small changes to surface potentials can lead to drastic shape differences (Figure 3c). This finding can explain the high cubicity reported for particle growing when hydrogen permeates fuel cell membranes towards the cathode, as hydrogen preferentially adsorb on the Pt(100) face [43]. Further, this knowledge was applied to develop a non-contact printing technology that uses only simple assembly rules (voltages and local illumination

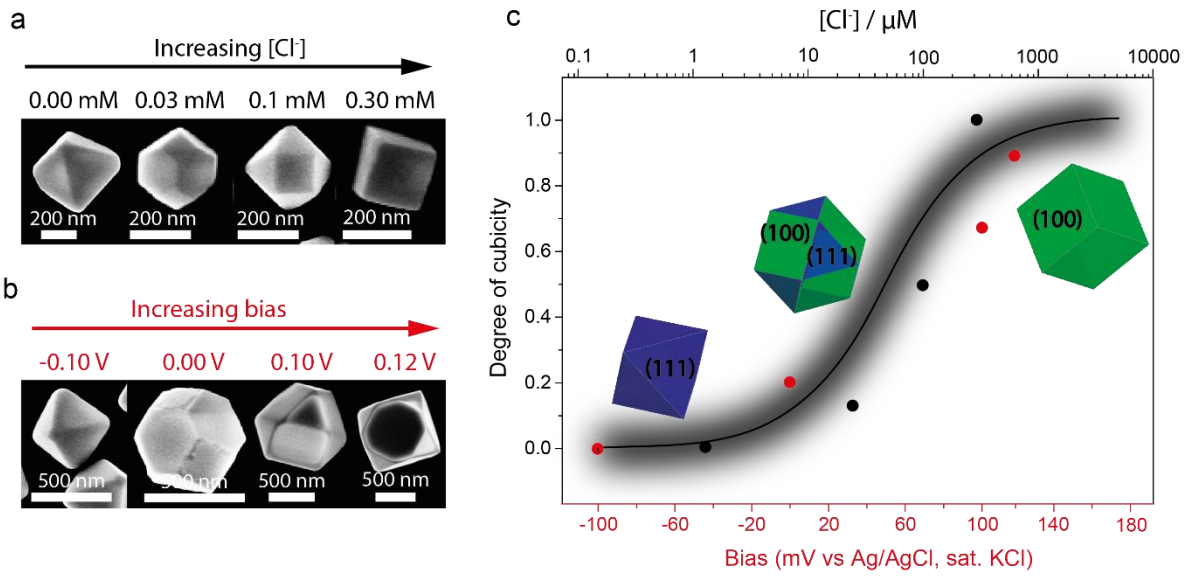

Figure 3. Tuning surface energy with bias-dependent anisotropic adsorption of charged species. (a) SEM data showing the change of crystal shape for a constant electrolysis potential but with changes to the bulk concentration of chloride ions. (b) Evolution of the crystal shape in response to an increased anodic bias under a fixed chloride ions concentration. (c) Plots of the "degree of cubicity" *versus* bias (or *versus* concentration, top *x*-axis) under constant illumination based on a Langmuir isotherm (solid line). Reprinted from Ref. [28], copyright 2018, with permission from the American Chemical Society.

density of a semiconductor electrode) for anti-counterfeiting applications [42].

It is a speculation, but not unreasonable, that as for the electrosynthesis of Cu_2O particles described above, differences in the electroadsorption bias of charged species, perhaps due to differences in the crystal's potential of zero charge (pzc) [44], could account for the remarkably different facet-specific rate in the electrografting of organic cations on metals and semiconductors [45]. As shown in Figure 4a–c, anisotropic etching of Si(100) wafers with hydroxide-containing solutions leads to a textured surface that exposes an array of Si(111) pyramids. In such a system, the presence or absence, as well as the number and density of ⟨211⟩ facets on a Si(100) crystal can be systematically adjusted. The reduction of a diazonium salt monolayer-forming molecule (o-dianisidine bis(diazotized) zinc double salt, **bis-diazo** in short), followed by its irreversible chemisorption, is favored on Si(111), with a ~200 mV separation between two clear reductive waves visible in Figure 3d. As both facets are simultaneously present on the same electrode, ambiguities potentially arising from a drifting

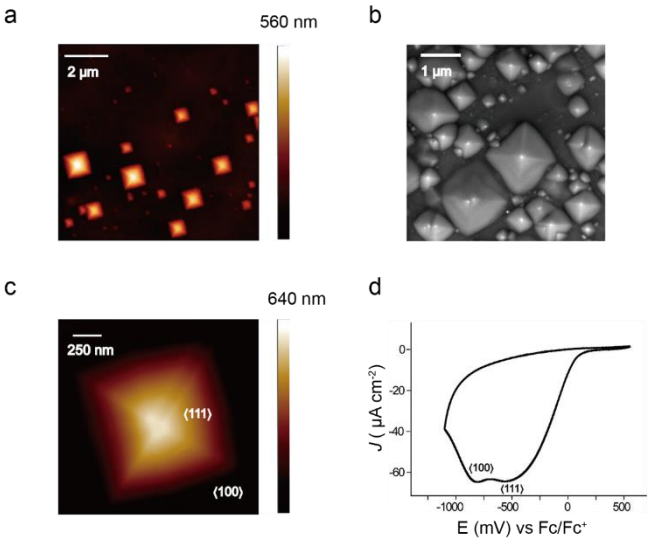

Figure 4. **Facet-dependent electro-grafting of organic films on textured silicon**. (a) AFM topography image and (b) SEM image of a Si(100) electrode exposing an array of Si(111) pyramids. (c) AFM image of a single Si(111) pyramid protruding from a Si(100) surface. (d) Electrochemical reduction wave of **bis-diazo** (1 mM *o*-dianisidine bis(diazotized) zinc double salt, with 0.1 M Bu_4NPF_6 in a 1:49 v/v DMSO/ACN mixture) on the sample presented in (a) and (b). The scan rate was 50 mV /s. Reprinted with minor changes from Ref. [45], copyright (2019), with permission from the American Chemical Society.

reference electrode are prevented. The answer to the question of whether different rates are due to a favored adsorption of **bis-diazo** on Si(111) prior to the electrochemical step, perhaps due to differences in pzc between Si(100) and Si(111), or whether differences in surface conductivities are involved, will require further experiments. What is certain is that Si(111) pyramids are more conductive than the Si(100) plane from which the protrude [46], and that different facets of the same material can have significantly different pzc [44,47]. Furthermore, electrical conductivity peaks on the pyramid apex, perhaps because a relatively small amount of charge at the tip of an asperity leads to a large electric field outside the solid [48]. Whether electrochemical currents also peak at the convex pyramid apex, and/or in proximity of the (111)–(100) planes intersection, where a concave curvature should lead to a thinner space charge [49], as exploited in the formation of porous silicon [50], remain also to be experimentally determined.

A similar scenario to the facet-dependent **bis-diazo** electroadsorption described above has also been recently reported for a form of gallium(III) trioxide, β-Ga_2O_3. This is a semiconductor with an extremely high breakdown field, nearly 8 MV/cm, which is also transparent, hence an

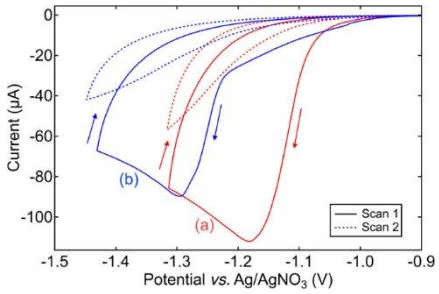

Figure 5. Facet-resolved electrochemistry on transparent electrodes. Cathodic electrografting of an aryl diazonium salt (NBD, 2 mM in acetonitrile with 0.1 M $[Bu_4N]BF_4$) through a cyclic voltammetry experiment (50 mV/s) on either β-Ga_2O_3(201) (red trace) or β-Ga_2O_3(010) (blue trace). Reprinted with minor changes from Ref. [52], copyright (2021), with permission from the American Chemical Society.

actively investigated alternative to the more commonly used and amorphous indium tin oxide [51]. The monoclinic crystal structure of β-Ga_2O_3 is highly anisotropic, to the point that for example its optical bandgap measured along the [010] direction is 4.57 eV, while it reaches 4.71 eV along the [201]. In a recent and very elegant study [52], Allen and co-workers have demonstrated that organic monolayers are a viable means to predictably tune the band bending of *β*-Ga_2O_3, to the point of achieving a downward band bending for a material that is normally strongly depleted in electrons. In this work there is clear implicit evidence of different crystal facets of β-Ga_2O_3 leading to very different electrografting rates. As shown in Figure 5, the electrochemical grafting (reduction followed by chemisorption) of 4-nitrobenzenediazonium (NBD) [as tetrafluoroborate salt] is faster on the (210) facet. It remains to be explored whether the slower rate observed on *β*-Ga_2O_3(010) may be due to the its higher electron affinity, and/or to the stronger upward band bending of the (010) compared to the (201) facet [53].

Facet-dependent electrocatalysis application

Hydrogen is a clean and renewable energy source and its production by hydrogen evolution reaction (HER) during water electrolysis is perhaps one of the most actively researched electrochemical reactions. Both computations and experiments indicate that the HER can be strongly facet dependent [54,55]. Transition metal phosphides (TMP) are non-precious metal compounds alternative to platinum. The relationship between crystal facets and HER rates has been investigated on alternative crystallographic facets of the same material: single crystals of

iron-phosphide (FeP) and monoclinic nickel-diphosphide (m-NiP_2) [56]. Experimental results suggest that the anisotropy of the catalytic activity is a feature for HER on TMPs. For FeP, a metallic material, the most active crystal facet was the ⟨010⟩, followed by ⟨101⟩, ⟨111⟩, and ⟨011⟩ is the least active facet. For m-NiP_2, a semiconductor, the ⟨100⟩ facet showed the highest activity, ⟨121⟩ and ⟨101⟩ were a little lower in activity, and ⟨111⟩ was the least active. These data agrees well with DFT calculations, which indicate that the energy of H-binding is strongly facet-dependent. Further, the experiments–calculations correlation is particularly strong for H-binding energies on P on specific surface terminations, pointing to the need of improving our ability to perform and map electrochemistry on single crystals [56]. An interesting consequence of these results is that they weaken the generally held assumption, for transition-metal phosphides, of surface restructuring during the reaction. If this was the case the structure of the bulk catalysts would not particularly matter, as restructuring would occur in situ.

Notably, findings similar to those discussed above are also available for CO_2 reduction [57], with electrochemical currents for the reduction of CO_2 being one order of magnitude greater on Au(110) than on both Au(111) and Au(100).

Summary and perspective

Assisted by recent developments in areas such as redox imaging [58,59], spatially resolved electrochemistry [60], electrochemistry at the nanoscale [61,62], and electrochemistry in confined spaces [63], there is a growing awareness of the anisotropic catalytic activity of alternative facets of technological materials such as silicon, Cu_2O, GaAs, InN, Ag_2O, and β-Ga_2O_3. Facet-resolved electrochemistry is developing rapidly, and it has already had a fundamental and practical impact on semiconductor electrochemistry, redox lithography, electrocatalysis, particle and film growth. There are mature theoretical models that can explain the available experimental data, as well as guide the rational design of new materials and optimized electrode surfaces that will contribute to the global challenge of integrating renewable electricity into chemical manufacturing, that is, to progressively replace conventional molecular reactants with electricity towards a sustainable chemical industry.

Conflict of interest statement

The authors declare that they have no known competing financial interests or personal relationships that could have appeared to influence the work reported in this paper.

Acknowledgements

S.C. acknowledges support from the Australian Research Council (grants no. FT190100148, DP190100735).

References

Papers of particular interest, published within the period of review, have been highlighted with an asterisk (*).

1. Gileadi E: *Electrode kinetics for chemists, chemical engineers and materials scientists.* Wiley-VCH Verlag GmbH, New York (1993).

2. Bard AJ, Faulkner LR: *Electrochemical methods : Fundamentals and applications.* John Wiley & Sons, Hoboken (2007).

3. Bangle RE, Schneider J, Conroy DT, Aramburu-Trošelj BM, Meyer GJ: **Kinetic evidence that the solvent barrier for electron transfer is absent in the electric double layer.** *J Am Chem Soc* (2020) **142**:14940–14946.

4. Gonçales VR, Lian J, Gautam S, Hagness D, Yang Y, Tilley RD, Ciampi S, Gooding JJ: **Heterojunctions based on amorphous silicon: A versatile surface engineering strategy to tune peak position of redox monolayers on photoelectrodes.** *J Phys Chem C* (2020) **124**:836–844.

5. Hurth C, Li C, Bard AJ: **Direct probing of electrical double layers by scanning electrochemical potential microscopy.** *J Phys Chem C* (2007) **111**:4620–4627.

6. Darwish N, Eggers PK, Ciampi S, Tong Y, Ye S, Paddon-Row MN, Gooding JJ: **Probing the effect of the solution environment around redox-active moieties using rigid anthraquinone terminated molecular rulers.** *J Am Chem Soc* (2012) **134**:18401–18409.

7. Favaro M, Jeong B, Ross PN, Yano J, Hussain Z, Liu Z, Crumlin EJ: **Unravelling the electrochemical double layer by direct probing of the solid/liquid interface.** *Nat Commun* (2016) **7**:12695.

8. Quaino P, Juarez F, Santos E, Schmickler W: **Volcano plots in hydrogen electrocatalysis - uses and abuses.** *Beilstein J Nanotechnol* (2014) **5**:846–854.

9. Roy N, Sohn Y, Pradhan D: **Synergy of low-energy {101} and high-energy {001} tio$_2$ crystal facets for enhanced photocatalysis.** *ACS Nano* (2013) **7**:2532–2540.

10. Wallace SK, McKenna KP: **Facet-dependent electron trapping in tio_2 nanocrystals.** *J Phys Chem C* (2015) **119**:1913–1920.

11. Asif AH, Rafique N, Hirani RAK, Wu H, Shi L, Zhang S, Wang S, Yin Y, Saunders M, Sun H: **Morphology/facet-dependent photo-fenton-like degradation of pharmaceuticals and personal care products over hematite nanocrystals.** *Chem Eng J* (2022) **432**:134429.

12. Luo Y, Deng Y, Guan L, Ye L, Guo X, Luo A: **Effect of grain size and crystal orientation on the corrosion behavior of as-extruded mg-6gd-2y-0.2zr alloy.** *Corros Sci* (2020) **164**:108338.

13. Toyoda T, Yindeesuk W, Kamiyama K, Hayase S, Shen Q: **Adsorption and electronic structure of cdse quantum dots on single crystal zno: A basic study of quantum dot-sensitization system.** *J Phys Chem C* (2016) **120**:16367–16376.

*14. Yang Y, Zeng J, Shu Y, Gao Q: **Revealing facet effects of palladium nanocrystals on electrochemical biosensing.** *ACS Appl Mater Interfaces* (2020) **12**:15622–15630. Facet-dependent hydrogen peroxide biosensing. Preferential binding of hydroxyls radicals on Pt(100) harnessed for glucose detection and design of efficient sensing platforms based on noble metals nanocrystals.

15. Yu X-Y, Meng Q-Q, Luo T, Jia Y, Sun B, Li Q-X, Liu J-H, Huang X-J: **Facet-dependent electrochemical properties of co_3o_4 nanocrystals toward heavy metal ions.** *Sci Rep* (2013) **3**:2886.

*16. Zhang S, Ferrie S, Peiris CR, Lyu X, Vogel YB, Darwish N, Ciampi S: **Common background signals in voltammograms of crystalline silicon electrodes are reversible silica-silicon redox chemistry at highly conductive surface sites.** *J Am Chem Soc* (2021) **143**:1267–1272. First experimental demonstration of reversible electrochemical silica-to-silicon conversion at room temperature. Discovery that redefines for silicon the potential window free from redox parasitic signals, and therefore suitable to study surface reactions by means of electroanalytical methods.

17. Mankin MN, Day RW, Gao R, No Y-S, Kim S-K, McClelland AA, Bell DC, Park H-G, Lieber CM: **Facet-selective epitaxy of compound semiconductors on faceted silicon nanowires.** *Nano Lett* (2015) **15**:4776–4782.

18. Tan C-S, Zhao Y, Guo R-H, Chuang W-T, Chen L-J, Huang MH: **Facet-dependent surface trap states and carrier lifetimes of silicon.** *Nano Lett* (2020) **20**:1952–1958.

19. Kuo CH, Yang YC, Gwo S, Huang MH: **Facet-dependent and au nanocrystal-enhanced electrical and photocatalytic properties of au-cu_2o core-shell heterostructures.** *J Am Chem Soc* (2011) **133**:1052–1057.

20. Tachikawa T, Yamashita S, Majima T: **Evidence for crystal-face-dependent tio_2 photocatalysis from single-molecule imaging and kinetic analysis.** *J Am Chem Soc* (2011) **133**:7197–7204.

21. Judd CJ, Haddow SL, Champness NR, Saywell A: **Ullmann coupling reactions on ag(111) and ag(110); substrate influence on the formation of covalently coupled products and intermediate metal-organic**

structures. *Sci Rep* (2017) **7**:14541.

*22. Torquato LDM, Pastrian FAC, Perini JAL, Irikura K, de L. Batista AP, de Oliveira-Filho AGS, Córdoba de Torresi SI, Zanoni MVB: **Relation between the nature of the surface facets and the reactivity of Cu_2O nanostructures anchored on TiO_2nt@pda electrodes in the photoelectrocatalytic conversion of CO_2 to methanol.** *Appl Catal, B* (2020) **261**:118221.
Optical properties and photocatalytic performance of Cu_2O nanostructures are facet-dependent. Superior catalytic activity of {100} facets attributed to a larger density of oxygen vacancies, promoting the activation of CO_2 for its conversion to methanol.

23. Ball P: **Silicon still supreme.** *Nat Mater* (2005) **4**:119–119.

24. Pharr M, Zhao K, Wang X, Suo Z, Vlassak JJ: **Kinetics of initial lithiation of crystalline silicon electrodes of lithium-ion batteries.** *Nano Lett* (2012) **12**:5039–5047.

25. Zhang S, Ferrie S, Lyu X, Xia Y, Darwish N, Wang Z, Ciampi S: **Absence of a relationship between surface conductivity and electrochemical rates: Redox-active monolayers on si(211), si(111), and si(110).** *J Phys Chem C* (2021) **125**:18197–18203.

26. Vogel YB, Gooding JJ, Ciampi S: **Light-addressable electrochemistry at semiconductor electrodes: Redox imaging, mask-free lithography and spatially resolved chemical and biological sensing.** *Chem Soc Rev* (2019) **48**:3723–3739.

*27. Tan C-S, Hsieh P-L, Chen L-J, Huang MH: **Silicon wafers with facet-dependent electrical conductivity properties.** *Angew Chem Int Ed* (2017) **56**:15339–15343.
Microscopic conductivity measurements reveal different degrees of conduction band bending hence different barrier heights to current flow for readily available but entirely underexploited Si(211) wafers.

28. Vogel YB, Zhang J, Darwish N, Ciampi S: **Switching of current rectification ratios within a single nanocrystal by facet-resolved electrical wiring.** *ACS Nano* (2018) **12**:8071–8080.

29. Tan C-S, Chen L-J, Huang MH: **Large facet-specific built-in potential differences affecting trap state densities and carrier lifetimes of gaas wafers.** *J Phys Chem C* (2020) **124**:21577–21582.

30. Liu H, Ma X, Chen Z, Li Q, Lin Z, Liu H, Zhao L, Chu S: **Controllable synthesis of [11−2−2] faceted inn nanopyramids on zno for photoelectrochemical water splitting.** *Small* (2018) **14**:1703623.

31. Chen Y-J, Chiang Y-W, Huang MH: **Synthesis of diverse Ag_2O crystals and their facet-dependent photocatalytic activity examination.** *ACS Appl Mater Interfaces* (2016) **8**:19672–19679.

32. Allongue P, Henry de Villeneuve C, Morin S, Boukherroub R, Wayner DDM: **The preparation of flat h–si(111) surfaces in 40% NH_4F revisited.** *Electrochim Acta* (2000) **45**:4591-4598.

33. Ciampi S, Harper JB, Gooding JJ: **Wet chemical routes to the assembly of organic monolayers on silicon**

surfaces via the formation of si-c bonds: Surface preparation, passivation and functionalization. *Chem Soc Rev* (2010) **39**:2158–2183.

34. Fabre B: **Functionalization of oxide-free silicon surfaces with redox-active assemblies.** *Chem Rev* (2016) **116**:4808–4849.

35. Nohira T, Yasuda K, Ito Y: **Pinpoint and bulk electrochemical reduction of insulating silicon dioxide to silicon.** *Nat Mater* (2003) **2**:397–401.

36. Vogel YB, Zhang L, Darwish N, Gonçales VR, Le Brun A, Gooding JJ, Molina A, Wallace GG, Coote ML, Gonzalez J, Ciampi S: **Reproducible flaws unveil electrostatic aspects of semiconductor electrochemistry.** *Nat Commun* (2017) **8**:2066.

37. Wu YF, Kashi MB, Yang Y, Goncales VR, Ciampi S, Tilley RD, Gooding JJ: **Light-activated electrochemistry on alkyne-terminated si(100) surfaces towards solution-based redox probes.** *Electrochim Acta* (2016) **213**:540–546.

38. Zhang L, Vogel YB, Noble BB, Goncales VR, Darwish N, Brun AL, Gooding JJ, Wallace GG, Coote ML, Ciampi S: **Tempo monolayers on si(100) electrodes: Electrostatic effects by the electrolyte and semiconductor space-charge on the electroactivity of a persistent radical.** *J Am Chem Soc* (2016) **138**:9611–9619.

39. Huang L, Zhang X, Wang Q, Han Y, Fang Y, Dong S: **Shape-control of pt-ru nanocrystals: Tuning surface structure for enhanced electrocatalytic methanol oxidation.** *J Am Chem Soc* (2018) **140**:1142–1147.

40. Li B, Yan Y, Shen C, Yu Y, Wang Q, Liu M: **Extraordinary lithium ion storage capability achieved by sno_2 nanocrystals with exposed {221} facets.** *Nanoscale* (2018) **10**:16217–16230.

41. Anwer S, Bharath G, Iqbal S, Qian H, Masood T, Liao K, Cantwell WJ, Zhang J, Zheng L: **Synthesis of edge-site selectively deposited au nanocrystals on tio_2 nanosheets: An efficient heterogeneous catalyst with enhanced visible-light photoactivity.** *Electrochim Acta* (2018) **283**:1095–1104.

42. Vogel YB, Gonçales VR, Al-Obaidi L, Gooding JJ, Darwish N, Ciampi S: **Nanocrystal inks: Photoelectrochemical printing of cu_2o nanocrystals on silicon with 2d control on polyhedral shapes.** *Adv Funct Mater* (2018) **28**:1804791.

43. Ferreira PJ, Shao-Horn Y: **Formation mechanism of pt single-crystal nanoparticles in proton exchange membrane fuel cells.** *Electrochem Solid-State Lett* (2007) **10**:B60-B63.

44. Su S, Siretanu I, van den Ende D, Mei B, Mul G, Mugele F: **Facet-dependent surface charge and hydration of semiconducting nanoparticles at variable ph.** *Adv Mater* (2021) **33**:2106229.

*45. Peiris CR, Vogel YB, Le Brun AP, Aragonès AC, Coote ML, Díez-Pérez I, Ciampi S, Darwish N: **Metal–single-molecule–semiconductor junctions formed by a radical reaction bridging gold and silicon electrodes.**

J Am Chem Soc (2019) **141**:14788–14797.
Evidence of different electrografting rates of diazonium salts on Si(100) and Si(111). Textured Si(100) surfaces presenting arrays of Si(111) pyramids as in-situ controls.

*46. Ferrie S, Darwish N, Gooding JJ, Ciampi S: **Harnessing silicon facet-dependent conductivity to enhance the direct-current produced by a sliding schottky diode triboelectric nanogenerator.** *Nano Energy* (2020) **78**:105210.
Electrical conductivity peaks at convex boundaries between identical crystal planes (larger fields outside the material) and at concave boundaries between dissimilar planes (possibly due to a thinner space charge).

47. Łukomska A, Sobkowski J: **Potential of zero charge of monocrystalline copper electrodes in perchlorate solutions.** *J Electroanal Chem* (2004) **567**:95–102.

48. Lazić P, Persson BNJ: **Surface-roughness–induced electric-field enhancement and triboluminescence.** *EPL* (2010) **91**:46003–46007.

49. Zhang XG: **Mechanism of pore formation on n-type silicon.** *J Electrochem Soc* (1991) **138**:3750–3756.

50. Zhang XG, Collins SD, Smith RL: **Porous silicon formation and electropolishing of silicon by anodic polarization in hf solution.** *J Electrochem Soc* (1989) **136**:1561–1565.

51. Vogel YB, Evans C, Belotti M, Xu L, Russell I, Yu L-J, Fung A, Hill N, Darwish N, Gonçales V, Coote ML *et al*: **The corona of a surface bubble promotes electrochemical reactions.** *Nat Commun* (2020) **11**:6323.

*52. Carroll LR, Martinez-Gazoni RF, Gaston N, Reeves RJ, Downard AJ, Allen MW: **Bidirectional control of the band bending at the ($2\bar{0}1$) and (010) surfaces of β-ga_2o_3 using aryldiazonium ion and phosphonic acid grafting.** *ACS Appl Electron Mater* (2021) **3**:5608–5620.
Facet-dependent electrografting of 4-nitrobenzenediazonium and realization of downward band bending by surface chemistry in a material that is normally strongly electron-depleted.

53. Hou C, Gazoni RM, Reeves RJ, Allen MW: **Direct comparison of plain and oxidized metal schottky contacts on β-ga_2o_3.** *Appl Phys Lett* (2019) **114**:033502.

54. Hu HX, Chang B, Sun XC, Huo Q, Zhang BG, Li YL, Shao YL, Zhang L, Wu YZ, Hao XP: **Intrinsic properties of macroscopically tuned gallium nitride single-crystalline facets for electrocatalytic hydrogen evolution.** *Chem Eur J* (2019) **25**:10420–10426.

*55. Choi M, Siepser NP, Jeong S, Wang Y, Jagdale G, Ye XC, Baker LA: **Probing single-particle electrocatalytic activity at facet-controlled gold nanocrystals.** *Nano Lett* (2020) **20**:1233–1239.
Nanoscale voltammetric mapping of individual nanocrystals demonstrating superior reductive electrocatalysis by Au cubes over Au octahedra.

*56. Owens-Baird B, Sousa JPS, Ziouani Y, Petrovykh DY, Zarkevich N, Johnson DD, Kolen'ko YV, Kovnir K: **Crystallographic facet selective her catalysis: Exemplified in fep and nip_2 single crystals.** *Chem Sci* (2020)

11:5007–5016.
Experimental demonstration of facet-dependent HER on transition metal phosphides. Evidence of preferred H-binding on P of specific surface terminations. Challenges the tenet of surface restructuring during the reaction.

*57. Marcandalli G, Villalba M, Koper MTM: **The importance of acid-base equilibria in bicarbonate electrolytes for co_2 electrochemical reduction and co reoxidation studied on au(hkl) electrodes.** *Langmuir* (2021) **37**:5707–5716.
Study on monocrystalline gold electrodes demonstrating that, for the ectrocatalysis of CO_2 electrochemical reduction CO, Au(110) is the most active surface. Elucidates the importance of the bicarbonate electrolytes and acid–base equilibria on this particular electroreduction.

58. Vogel YB, Darwish N, Ciampi S: **Spatiotemporal control of electrochemiluminescence guided by a visible light stimulus.** *Cell Rep Phys Sci* (2020) **1**:100107.

59. Rapino S, Treossi E, Palermo V, Marcaccio M, Paolucci F, Zerbetto F: **Playing peekaboo with graphene oxide: A scanning electrochemical microscopy investigation.** *Chem Commun* (2014) **50**:13117–13120.

60. Fiorani A, Han D, Jiang D, Fang D, Paolucci F, Sojic N, Valenti G: **Spatially resolved electrochemiluminescence through a chemical lens.** *Chem Sci* (2020) **11**:10496–10500.

61. Zhao Y, Bouffier L, Xu G, Loget G, Sojic N: **Electrochemiluminescence with semiconductor (nano)materials.** *Chem Sci* (2022) **13**:2528–2550.

62. Verlato E, Barison S, Einaga Y, Fasolin S, Musiani M, Nasi L, Natsui K, Paolucci F, Valenti G: **Co_2 reduction to formic acid at low overpotential on bdd electrodes modified with nanostructured ceo_2.** *J Mater Chem A* (2019) **7**:17896–17905.

63. Andronescu C, Masa J, Tilley RD, Gooding JJ, Schuhmann W: **Electrocatalysis in confined space.** *Curr Opin Electrochem* (2021) **25**:100644.

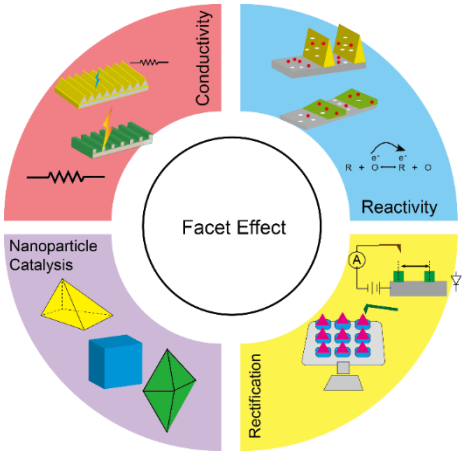
Conductivity
Reactivity
Facet Effect
Nanoparticle
Catalysis
Rectification